STUDY OF OXYGEN EVOLUTION REACTION ON IRON GROUP-BASED ELECTRODEPOSITED MULTICOMPONENT CATALYSTS IN ALKALINE MEDIA. PART I: INFLUENCE OF THE COMPOSITION

Vasil Bachvarov[1], Marina Arnaudova[1], Elefteria Lefterova[2], Rashko Rashkov[1]

[1]*Institute of Physical Chemistry, Bulgarian Academy of Sciences*
11 Acad. G. Bonchev Str., 1113 Sofia, Bulgaria
[2]*Institute of Electrochemistry and Energy Systems*
Bulgarian Academy of Sciences, 10 Acad. G. Bonchev Str.
1113 Sofia, Bulgaria
E-mail address: rasho@ipc.bas.bg

Received 18 March 2022
Accepted 06 April 2022

ABSTRACT

Iron group metal-based electrocatalysts are a low-cost and highly effective alternative to precious metals in water splitting. Herein, catalysts for oxygen evolution reaction (OER) obtained from multicomponent alloys by means of the facile electrochemical method are reported. OER electrocatalytic properties of NiCoFeMo, NiFeCoP, and NiCoFeW alloys are studied by polarization curves in 6M KOH. Tafel slopes and OER overpotentials are determined at quasi-stationary conditions (0.1 mV s^{-1} scan rate). For comparison purposes also binary NiW and NiMo alloys, and a ternary NiMoW alloy are examined. Results show dramatically lower OER overpotential values (by over 200 mV for $i = 100$ mA cm^{-2}) for quaternary systems compared to pure nickel, and binary and ternary systems. This behavior can be attributed to higher Fe- and Co-doping to the nickel matrix, and possibly, to the mixed (oxy)hydroxides formed during anodic polarization, responsible for high OER efficiency. The best OER catalytic activity is demonstrated by $Ni_{56}Fe_{21}Co_{13}P_{10}$ alloy attributable to the presence of phosphorous.

Keywords: Oxygen evolution reaction, electrocatalytic activity, electrodeposition, amorphous alloys, NiFeCoP.

INTRODUCTION

A basic method for obtaining high-purity hydrogen is water splitting. Process rate-limiting reaction is the anodic oxygen evolution. Electrode requirements involve good catalytic activity, corrosion resistance, mechanical stability, and price - the lower is the better. Development of alkaline electrolyzer with a polymer anion exchange membrane allows for replacing the expensive anode materials with materials based on non-precious metals. Possible candidates for oxygen evolution reaction (OER) meeting these requirements are transition metals such as Ni, Fe, Co, and their alloys [1 - 5], hydroxides [6, 7] and oxides [6, 8 - 10]. NiCo alloys are much more active than a pure Ni electrode. With the increase in alloy Co content, alloy electrocatalytic activity rises [1]. NiCo alloys containing 30 - 50 % Co have shown lower overpotential values for OER than the nickel electrode [3]. The good OER catalytic behavior of cobalt-containing catalysts has been attributed to the formation of surface cobalt oxides and hydroxides [11, 12]. It has been assumed that Fe-doping of Ni hydroxides leads to building up more active sites, which in turn increased OER activity [7]. Amorphous NiFe oxyhydroxide obtained *in situ* on NiFe alloy nanowire surface has also determined to be a highly active phase for oxygen evolution [13].

Furthermore, Fe insertion increases NiOOH conductivity and affects NiOOH electronic structure by inducing a partial charge transfer activation effect on Ni, resulting in OER activity boost via formation of a $Ni_{1-x}Fe_xOOH$ layer [14, 15].

A nanoscale NiFeP electrocatalyst synthesized by the sol-gel method has shown better OER activity than Ni_2P and FeP alone [16], which suggests that the more components in the alloys, the higher catalytic activity of the material. For example, ternary amorphous $Ni_{0.51}Co_{0.49}P$ alloys exhibit better OER catalytic properties compared

to binary NiP and CoP alloys [17]. Darband et al. [18] have established that the better catalytic activity of ternary NiFeCo alloys compared to binary Ni-Co and Ni-Fe is attributable to the synergistic effect between Ni, Fe and Co. Moreover, Ni-Fe-Co catalyst is stable and in an alkaline environment, maintains its activity for long [19].

Phosphides [20, 21] and phosphates [22] formed on the surface of iron and cobalt-nickel matrices have demonstrated excellent OER catalytic properties. This opens up an opportunity for their commercial application as electrodes for water splitting systems instead of the precious metal-based electrodes. In a study of binary and ternary Ni, Fe, Co with Mo alloys, Plata-Torres et al. have established an improved catalytic activity with Ni and/or Mo content increase [2].

Presence of tungsten in Mn-Mo-W [23] and Ni-Fe-W LDH [24] oxide anodes boosts electrical conductivity of oxide materials and improves catalytic efficiency. However, the different tungsten content in Ni-W alloys affects their catalytic activity [25].

All this gives a reason to deduce that catalytic materials of an enhanced OER activity can be obtained by combining transition elements in 2 and 3 component alloys (Mo, Co, W, Ni, and Fe). Along with a well-developed surface, these components incite a synergistic effect in such alloys, their oxides and hydroxides, thus contributing to a better catalytic activity compared to the pure metals.

In our previous works we have studied the preparation, composition and catalytic activity of some (3-4)-component alloys for hydrogen evolution reaction (HER) [26, 27]. We have explored the electrodeposited island structured 4-component alloys based on Ni-Fe-Co doped with Mo, W, and P. Integration of these materials as anodes in water electrolysis cells with anion exchange membrane leads to a better OER catalytic efficiency than the one of sol-gel deposited Pt anode [28]. These alloys exhibit a very promising potency and this prompting a more in-depth research on these systems.

The aim of the present paper is a detailed OER study of binary, ternary and quaternary alloys composed of Ni, Mo, Co, W, P, and Fe. We focus on the effect that composition of electrodeposited systems has on catalytic properties and on the rate-determining stage during OER. Alloys were electrochemically deposited on a smooth copper plate to avoid substrate surface influence in electrode catalytic behavior.

EXPERIMENTAL

Materials

All alloys were prepared by a galvanostatic electrodeposition in a thermostatic glass cell. Electrolytes used for the preparation of NiW, NiMo, NiMoW, NiCoFeMo, NiCoFeW and NiCoFeP alloys are presented in Table 1. Chemicals given in Table 1 were purchased from Sigma-Aldrich with minimum 99 % purity. Sodium citrate, β-alanine and glycine complexes were used to prevent nickel and iron ion hydrolysis, formation of respective hydroxides in the electrolyte, and to maintain Ni and Fe ions in a soluble state. The conditions for multicomponent alloys deposition (Table 2) were selected to ensure obtaining uniform coatings with good adhesion and particular composition.

A copper plate of a geometric area of 2 cm^{-2} was used as a substrate while a Ti-Pt mesh - as an anode. The copper plate was etched in a 1: 1 HCl solution preheated to 60-70°C to remove surface oxides. Then it was rinsed with distilled water.

Materials characterization

Structures of thin film produced were characterized by X-ray diffraction (XRD) using Philips PW 1050 diffractometer with $Cu_{K\alpha}$ radiation (l = 0.15418 nm) in the 30° - 95° 2θ range and scan step of 0.02°. Deposit component content was determined by Fischerscope® X-RAY system (X-ray fluorescence analysis; XRF) as average value of measurements in 9 points (three points at the bottom, middle and top of the sample, respectively). The morphology and the composition of the electroplated alloys were analyzed by scanning electron microscopy (SEM) with energy dispersion X-ray (EDX) JEOL JSM 6390 with INCA Oxford software.

Electrochemical measurements

A three-electrode cell equipped with a Luggin capillary at the working electrode connected to a Gamry (version 6.25) Potensiostat/Galvanostat was used. Alloy OER electrocatalytic activity was measured by the Linear Sweep Voltammetry (LSV) method at 0.1 mV s^{-1} scan rate. IR compensation experiments were performed in 6M KOH at room temperature. This medium was selected with the purpose of eventual use of systems studied as electrodes in an alkaline electrolyzer with a

Table 1. Electrolyte composition.

Composition g L^{-1}	Ni	NiW	NiMo	NiMoW	NiCoFeW	NiCoFeMo	NiCoFeP
Ni sulfamat (as Ni^{2+})	80	16	32	32	-	-	-
$Na_2WO_4.2H_2O$	-	30	-	24	30	-	-
$Na_2MoO_4.2H_2O$	-	-	6	6	-	12.5	-
$NiSO_4.7H_2O$	-	-	-	-	75	50	40
$NiCl_2.6H_2O$	10	-	-	-	12.5	10	40
$FeSO_4.7H_2O$	-	-	-	-	25	25	30
$CoSO_4.7H_2O$	-	-			25	50	5
$Na_3C_6H_5O_7.2H_2O$	-	90	72	72	125	125	-
H_3BO_3	30	-	-	-	-	-	-
β-alanine	-	-	-	-	-	-	
glycine	-	-	-	-	-	-	26
glycine	-	-	-	-	-	-	26
phosphorous content (50% H_3PO_4, $Na_2H_2PO_2$)	-	-	-	-	-	-	4.4

polymer anion exchange membrane, activated with 6M KOH. A Ti-Pt mesh was used as a counter electrode while Hg/HgO as a reference electrode. Each measurement continued until two successive polarization curves with a difference not higher than 3 mV were obtained. Before any LSV curve onset, the working electrode was subjected to galvanostatic polarization at an anodic current density of 100 mA cm^{-2} for 15 min to accelerate metal oxides and/or oxyhydroxides formation on the alloy surface.

The equilibrium potential for oxygen evolution (E^o_{rev}) was calculated as per equation (1)

$$E^o_{rev} = 1.230\ V - 0.059 \times pH \quad (1)$$

pH of 6 M KOH = 14.778. The potential of Hg/HgO vs. SHE was +0.12 V. Thus, the value of equilibrium potential for oxygen evolution was, E^o_{rev} = 0.238 V vs. Hg/HgO electrode. Overpotential (η) was determined as per equation (2):

$$\eta = E_{applied} - 0.238\,V \quad (2)$$

RESULTS AND DISCUSSION

Table 2 presents the conditions for obtaining the multicomponent systems studied using the electrochemical method. This method allows for fast production of materials and reproducibility of results. In addition, depending on the hydrodynamic regime employed, catalytic materials of different component ratios in the alloy can be produced from one and the same electrolyte. For instance, stirring NiCoFeMo electrolyte led to formation of $Mo_{35}Co_{29}Ni_{21}Fe_{15}$ alloy, while in the absence of stirring, $Mo_{34}Ni_{26}Co_{25}Fe_{15}$ coating was formed. A 100 rpm stirring of NiCoFeW electrolyte rendered deposition of $Co_{32}Fe_{30}W_{20}Ni_{18}$ alloy while in the absence of stirring, $Ni_{32}W_{31}Co_{19}Fe_{18}$ was formed. In a previous study it has been established that NiFeCoP alloys possess significant HER catalytic activity in 6M KOH [29]. For this reason, a $Ni_{56}Fe_{21}Co_{13}P_{10}$ alloy deposited at -10 A dm^{-2} was included in the current study.

XRD characterization

Fig. 1 presents XRD patterns for structural analysis

Table 2. Electrodeposition conditions.

Coatings	t, °C	pH	i_c, (A dm^{-2})	stirring (rpm)
Ni	50	4	4.5	-
$Ni_{80}W_{20}$	60	7	4.5	-
$NI_{90}Mo_{10}$	50	9	6	-
$Ni_{90}Mo_8W_2$	50	9	6	-
$Mo_{34}Ni_{26}Co_{25}Fe_{15}$	30	5.5	3	-
$Mo_{35}Co_{29}Ni_{21}Fe_{15}$	30	5.5	3	100
$Co_{32}Fe_{30}W_{20}Ni_{18}$	50	5.5	6	300
$Ni_{32}W_{31}Co_{19}Fe_{18}$	50	5.5	6	100

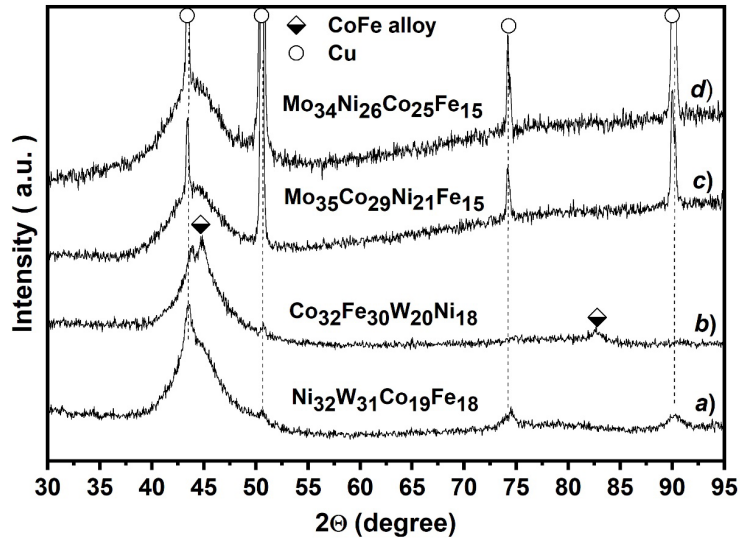

Fig. 1. XRD patterns of (a) $Ni_{32}W_{31}Co_{19}Fe_{18}$, (b) $Co_{32}Fe_{30}W_{20}Ni_{18}$, (c) $Mo_{35}Co_{29}Ni_{21}Fe_{15}$, (d) $Mo_{34}Ni_{26}Co_{25}Fe_{15}$.

of layers studied. Diffractograms of molybdenum coatings ($Mo_{34}Ni_{26}Co_{25}Fe_{15}$, $Mo_{35}Co_{29}Ni_{21}Fe_{15}$) showed a broad halo centered in the range of 44 - 45 degrees, corresponding to the strongest diffraction peak of pure Ni, Fe Co metals and of their alloys. The presence of a halo without distinct peaks was associated with the amorphous nature of the coatings. The relatively high peak intensity of the copper substrate in molybdenum coating diffractograms was an indication of a thin layer (less than 10 μm) deposition. Obviously, tungsten layers were thicker and the substrate peaks were of a very low intensity. Furthermore, tungsten coating $Ni_{32}W_{31}Co_{19}Fe_{18}$ was amorphous while $Co_{32}Fe_{30}W_{20}Ni_{18}$ layer contained a small amount of crystalline phase along with an amorphous one. The diffraction peaks at 44.86° and 82.67° were the closest to CoFe (PDF#44-1433) alloy. As it has been confirmed in a previous study, $Ni_{56}Fe_{21}Co_{13}P_{10}$ alloy is also amorphous [29]. The amorphous nature of quaternary alloys predetermines their nearly similar well-developed surface.

OER performance

OER electrocatalytic activity of the electrodeposited alloys was determined by LSV method. Overpotential versus current density logarithm is plotted in Fig. 2. Table 3 summarizes the main parameters of this dependence. A 10 wt. % Mo- and 20 wt. % W-doping in the nickel matrix (Fig. 2(a)) resulted in a negligible

Table 3. Parameters obtained by the analysis of the polarization curves presented on Fig. 2 (b_1 at low current density < 10 mA cm $^{-2}$ and b_2 at high current density > 10 mA cm $^{-2}$).

Samples	b V dec^{-1}	b_1 V dec^{-1}	b_2 V dec^{-1}	$\eta_{i=10}$ V	$\eta_{i=100}$ V	$i_{\eta400}$ mA cm^{-2}
1-Ni	0.131			0.578	0.720	0.47
2-$Ni_{90}W_{10}$	0.116			0.590	0.696	0.26
3-$Ni_{80}Mo_{20}$	0.129			0.592	0.707	0.47
4-$Ni_{90}Mo_8W_2$	0.126			0.577	0.686	0.53
5-$Mo_{34}Ni_{26}Co_{25}Fe_{15}$		0.059	0.116	0.365	0.469	26.7
6-$Ni_{32}W_{31}Co_{19}Fe_{18}$		0.054	0.065	0.366	0.432	31.2
7-$Mo_{35}Co_{29}Ni_{21}Fe_{15}$		0.050	0.064	0.353	0.416	57.7
8-$Co_{32}Fe_{30}W_{20}Ni_{18}$		0.050	0.058	0.353	0.411	61.7
9-$Ni_{56}W_{21}Co_{13}Fe_{10}$		0.044	0.067	0.329	0.393	128.2

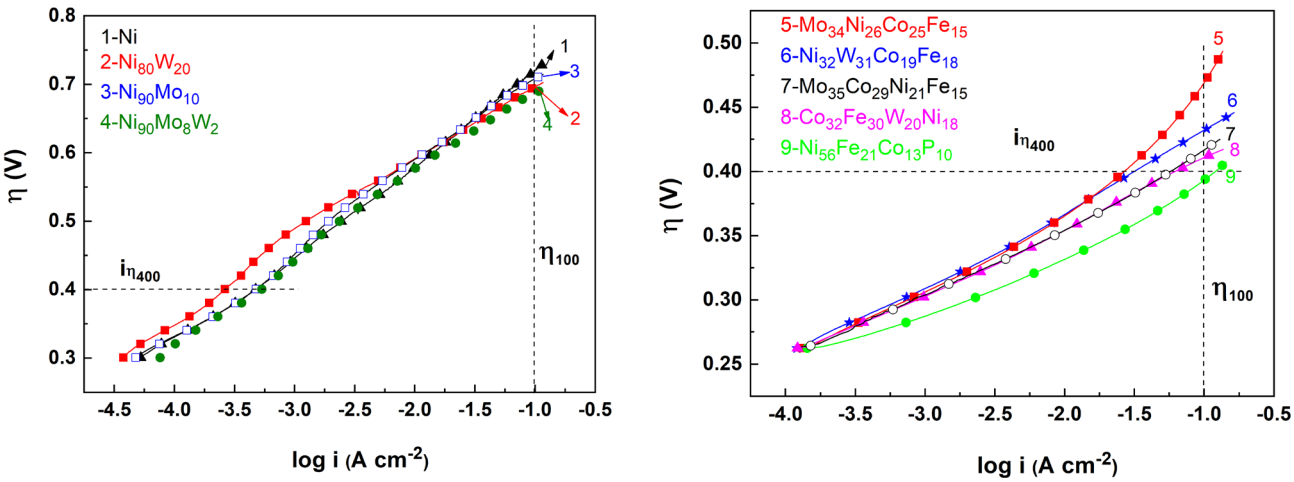

Fig. 2. Polarization curves in 6M KOH of (a) 1-Ni, 2-$Ni_{80}W_{20}$, 3-$Ni_{90}Mo_{10}$, 4-$Ni_{90}Mo_8W_2$ and (b) 5-$Mo_{34}Ni_{26}Co_{25}Fe_{15}$, 6-$Ni_{32}W_{31}Co_{19}Fe_{18}$, 7-$Mo_{35}Co_{29}Ni_{21}Fe_{15}$, 8-$Co_{32}Fe_{30}W_{20}Ni_{18}$, 9-$Ni_{56}Fe_{21}Co_{13}P_{10}$.

overpotential (η) reduction at a current density of 100 mA cm^{-2} (Table 3) as compared to pure nickel. The ternary $Ni_{90}Mo_8W_2$ alloy though containing smaller quantities of Mo and W maintained the decreasing trend in the value of $\eta_{i=100}$ (determined from Fig. 2(a), at lg i = -1). This corresponded with an improved catalytic activity compared to binary nickel alloys and pure nickel. Binary and ternary alloys, as well as pure nickel, were characterized by a Tafel slope b of about 120 mV dec^{-1} for both regions. However, quaternary alloys (Fig. 2(b), Table 3) showed a dramatically lower overpotential values (η for i = 100 mA cm^{-2}) between 250 and 320 mV compared to the pure nickel for OER. Tafel slopes b_1 and b_2 were about 40 and 60 mV dec^{-1}, respectively, indicating more favorable reaction kinetics.

Results in Fig. 2 and Table 3 pointed out that rising cobalt but reducing nickel content in quaternary Mo alloys 5 and 7 favored lower slope runs for both regions. Overpotential dropped by more than 50 mV (η for i = 100 mA cm^{-2}) and current density for OER at η = 400 mV went up from 26.7 to 57.7 mA cm^{-2}. The positive effect of Co and Fe was also obvious in alloys 6 and 8, both containing W. Lower Tafel slopes and smaller overpotential values (411 mV) and i′ = 400 (61.7 mA cm^{-2}) measured for $Co_{32}Fe_{30}W_{20}Ni_{18}$ determined the better OER catalytic activity compared to $Ni_{32}W_{31}Co_{19}Fe_{18}$ coatings. The better catalytic behavior of $Co_{32}Fe_{30}W_{20}Ni_{18}$ could be attributed to

the increased cobalt and iron content in the alloy. It has been established that increasing cobalt content in Ni-Co alloys improves electrocatalytic activity [1]. As claimed in [3], the best OER catalysts contain 30 % to 50 % Co. On the other hand, Fe-doping has been known to modify electron properties of the material, thus enhancing substantially OER catalytic activity [8]. It has been assumed that Fe-doping in Ni hydroxides leads to a higher number of active sites, prompting a higher OER activity [7].

Comparison of $\eta_i = 10$ and $\eta_i = 100$ values in Table 3 indicated that the lowest overpotential and, respectively, the best catalytic characteristics exhibited $Ni_{56}Fe_{21}Co_{13}P_{10}$ alloy. Within the entire overpotential range, the highest current density value was registered for this particular alloy, which corresponded with the lowest resistance in the oxygen generation process. It is reasonable to assume that the findings were associated with the nickel matrix iron and cobalt doping, and possibly, with the mixed (oxy)hydroxides formed during anodic polarization, the latter being typical for high OER efficiency. The presence of phosphorous in the $Ni_{56}Fe_{21}Co_{13}P_{10}$ alloy obtained electrochemically could also be a reason for the highest electrocatalytic activity observed. Qiong Zhang et al. have stipulated that transition metal phosphides may improve electron transport and respectively, electrocatalytic activity for OER [30].

The Tafel slope can be used to determine the rate-determining stage for the OER mechanism. There are two OER mechanisms suggested usually - Krasil`shichikov path [31] and electrochemical oxide pathway [32]. According to Jovich [33], at high anode potentials negatively charged intermediates (Krasil`shichikov path) would hardly exist on the surface, and therefore, the modified electrochemical oxide pathway is a more probable mechanism [33, 34]:

$$S + OH^- \rightarrow S\text{–}OH^* + e^- \quad 120\ mV\ dec^{-1} \quad (3)$$

$$S\text{–}OH^* \rightarrow S\text{–}OH \quad 60\ mV\ dec^{-1} \quad (4)$$

$$S\text{–}OH + OH^- \rightarrow S\text{–}O + H_2O + e^- \quad 40\ mV\ dec^{-1} \quad (5)$$

$$2S\text{–}O \rightarrow 2S + O_2 \quad (6)$$

where S means the active sites on the surface.

Pure nickel and alloys (2 - 4) showed slopes in both regions around 120 mV dec^{-1}, suggesting that the rate-determining step (RDS) was reaction (3) (see Table 3). At low current densities, the slopes varied between 44 mV dec^{-1} for $Ni_{56}Fe_{21}Co_{13}P_{10}$ and 59 mV dec^{-1} for $Mo_{34}Ni_{26}Co_{25}Fe_{15}$. These corresponded to, respectively, reactions (5) and (4), and were considered the limiting stages. The Tafel slope value for $Mo_{34}Ni_{26}Co_{25}Fe_{15}$ was 116 mV dec^{-1} observed at high current densities, i.e. OER mechanism was similar to the one for (pure) nickel, binary and ternary alloys. In this region, Tafel slopes for the other quaternary alloys (6 - 9, Table 3) were close to ~ 60 mV dec^{-1}, which corresponded to RDS reaction (4), i.e. chemical conversion from unstable to stable S – OH.

Tafel slope value deviations from the values calculated theoretically can be ascribed to several reasons: hydroxyl groups transport limitation, decrease in conductivity caused by adsorption of intermediates, active site blockage by bubbles due by oxygen evolution, etc.

SEM characterization

A typical globular structure after OER was observed in SEM images (Fig. 3), irrespective of whether Ni or Mo, or Co predominated in the alloys. No relation between the globule size, respectively, the surface and overpotential for OER, was established. For instance,

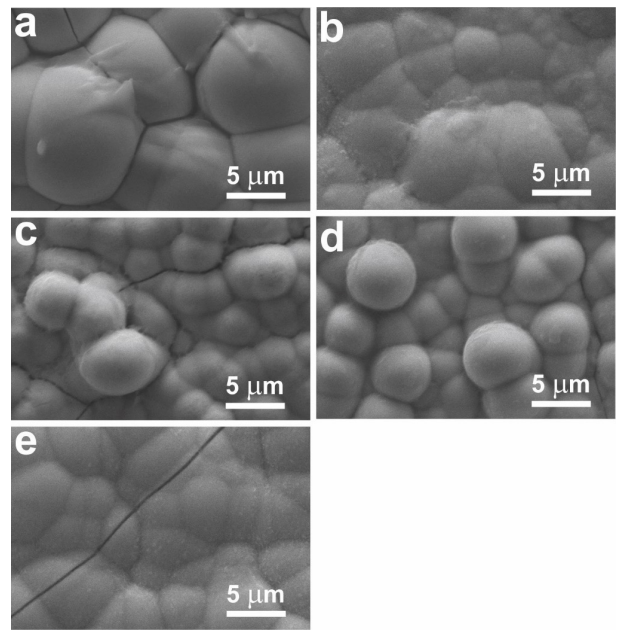

Fig. 3. SEM images of electrodeposited alloys (a) $Ni_{32}W_{31}Co_{19}Fe_{18}$, (b) $Co_{32}Fe_{30}W_{20}Ni_{18}$, (c) $Mo_{34}Ni_{26}Co_{25}Fe_{15}$, (d) $Mo_{35}Co_{29}Ni_{21}Fe_{15}$, (e) $Ni_{56}Fe_{21}Co_{13}P_{10}$.

molybdenum alloys, regardless of their identical morphology, (Fig. 3(c) and (d)), manifested higher than 50 mV difference in overpotential values. This is an indication that a good catalytic activity has to do more with valence state of alloy elements, possible compounds formed and electron interaction among them rather than the surface.

CONCLUSIONS

Oxygen evolution reaction in an alkaline medium was studied on iron group-based electrodeposited multicomponent alloys in the presence of Mo, W and P. The quaternary alloys showed lower OER overpotential values over 200 mV for i = 100 mA cm^{-2} corresponding to better catalytic properties than pure nickel and its binary and ternary alloys. This fact was associated, on the one hand, with an increase in the number of components and, on the other hand, with Co and Fe doping and, respectively, their content change in the alloys. The Tafel slope determined for them was about 60 mV dec^{-1}, which corresponded to a chemical conversion from unstable to stable S-OH as a rate-determining stage. The best OER catalytic activity was demonstrated by $Ni_{56}Fe_{21}Co_{13}P_{10}$ alloy with the smallest overpotential (0.393 V) and Tafel slope b_1 (0.044 V dec^{-1}).

However, further studies are required to determine the impact of surface and the electronic interaction between components in quaternary alloys so that differences in their OER catalytic efficiency can be explained. This is subject of further research work.

Acknowledgement

This work was supported by the Bulgarian Ministry of Education and Science under the National Research Programme "Low Carbon Energy for the Transport and Households" (E+), grant agreement D01-214/2018.

REFERENCES

1. B. Chi, J. Li, X. Yang, Y. Gong, N. Wang, Deposition of Ni-Co by cyclic voltammetry method and its electrocatalytic properties for oxygen evolution reaction, Int. J. Hydrogen Energy, 30, 2005, 29-34. https://doi.org/10.1016/j.ijhydene.2004.03.032
2. M. Plata-Torres, A.M. Torres-Huerta, M.A. Dominguez-Crespo, E.M. Arce-Estrada, C. Ramirez-Rodriguez, Electrochemical performance of crystalline Ni-Co-Mo-Fe electrodes obtained by mechanical alloying on the oxygen evolution reaction, Int. J. Hydrogen Energy, 32, 2007, 4142-4152. https://doi.org/10.1016/j.ijhydene.2007.05.023
3. F.J. Perez-Alonso, C. Adan, S. Rojas, M.A. Pena, J.L.G. Fierro, Ni-Co electrodes prepared by electroless-plating deposition. A study of their electrocatalytic activity for the hydrogen and oxygen evolution reactions, Int. J. Hydrogen Energy, 40, 2015, 51-61. https://doi.org/10.1016/j.ijhydene.2014.11.015
4. J.C.K. Ho, D.L. Piron, Active surface area in oxide electrodes by overpotential deposited oxygen species for the oxygen evolution reaction, J. App. Electrochem., 26, 1996, 515-21. https://doi.org/10.1007/BF01021975
5. F. Hu, Sh. Zhu, Sh. Chen, Y. Li, L. Ma, T. Wu, Y. Zhang, Ch. Wang, C. Liu, X.Yang, L. Song, X. Yang, Y. Xiong, Amorphous Metallic NiFeP: A Conductive bulk material achieving high activity for oxygen evolution reaction in both alkaline and acidic media, Adv. Mater., 29, 2017, 1-9. https://doi.org/10.1002/adma.201606570
6. J. Jiang, A. Zhang, L. Li, L. Ai, Nickel-cobalt layered double hydroxide nanosheets as high performance electrocatalyst for oxygen evolution reaction, J. Power Sources, 278, 2015, 445-51. https://doi.org/10.1016/j.jpowsour.2014.12.085
7. Z. Lu, W. Xu, W. Zhu, Q. Yang, X. Lei, J. Liu, Y. Li, X. Sun, X. Duan, Three-dimensional NiFe layered double hydroxide film for high-efficiency oxygen evolution reaction, Chem. Commun., 50, 2014, 6479-6482. https://doi.org/10.1039/C4CC0-1625D
8. M. Kumar, R. Awasthi, A.K. Pramanick, R.N. Singh, New ternary mixed oxides of Fe, Ni and Mo for enhanced oxygen evolution, Int. J. Hydrogen Energy, 36, 2011, 12698-12705. https://doi.org/10.1016/j.ijhydene.2011.07.029
9. E.B. Castro, C.A. Gervasi, Electrodeposited Ni-Co–oxide electrodes: characterization and kinetics of the oxygen evolution reaction, Int. J. Hydrogen Energy, 25, 12, 2000, 1163-1170. https://doi.org/10.1016/S0360-3199(00)00033-1
10. M.E.G. Lyons, R.L. Doyle, Oxygen evolution at oxidised iron electrodes: A tale of two slopes, Int.

J. Electrochem. Sci., 7, 2012, 9488-9501. https://doi.org/10.1021/ja502379c

11. K. Kordek, H. Yin, P. Rutkowski, H. Zhao, Cobalt-based composite films on electrochemically activated carbon cloth as high performance overall water splitting electrodes, Int. J. Hydrogen Energy, 44, 1, 2019, 23-33. https://doi.org/10.1016/-j.ijhydene.2018.02.095
12. T. Wang, Ch. Wang, Y. Jin, A. Sviripa, J. Liang, J. Han, Y. Huang, Q. Li, G. Wu, Amorphous Co-Fe-P nanospheres for efficient water oxidation, J. Mater. Chem., A 5 2017, 25378-25384. https://doi.org/10.1039/C7TA08720A
13. C. Liang , P. Zou , A. Nairan , Y. Zhang , J. Liu , K. Liu , S. Hu , F. Kang , H.J. Fan , C. Yang, Exceptional performance of hierarchical Ni-oxyhydroxide@ NiFe alloy nanowire array electrocatalysts for large current density water splitting, Energy and Environmental Sci., 13, 1, 2020, 86-95. https://doi.org/10.1039/C9EE02388G
14. L. Trotochaud, S.L. Young, J.K. Ranney, S.W. Boettcher, Nickel–iron oxyhydroxide oxygen-evolution electrocatalysts: The role of intentional and incidental iron incorporation, J. Am. Chem. Soc., 136, 18, 2014, 6744–6753. https://doi.org/10.1021/ja502379c
15. T. Rauscher, Ch.I. Bernäcker, U. Mühle, B. Kieback, L. Röntzsch, The effect of Fe as constituent in Ni-base alloys on the oxygen evolution reaction in alkaline solutions at high current densities, Int. J. Hydrogen Energy, 44, 13, 2019, 6392-6402. https://doi.org/10.1016/j.ijhydene.2019.01.182
16. Z. Liu, G. Zhang, K. Zhang, H. Liu, J. Qu, Facile dispersion of nanosized NiFeP for highly effective catalysis of oxygen evolution reaction, ACS Sustainable Chem. Eng., 6, 6, 2018, 7206-7211. https://doi.org/10.1021/acssuschemeng.8b00471
17. J. Yu, Q. Li, Y. Li, C.-Y. Xu, L. Zhen, V.P. Dravid, J. Wu, Ternary metal phosphide with triple-layered structure as a low-cost and efficient, electrocatalyst for bifunctional water splitting, Adv. Funct. Mater., 26, 2, 2016, 7644–7651. https://doi.org/10.1002/adfm.201603727
18. Gh.B. Darband, M. Aliofkhazraei, A.S. Rouhaghdam, Facile electrodeposition of ternary ni-fe-co alloy nanostructure as a binder free, cost-effective and durable electrocatalyst for high-performance overall water splitting, J. Coll. and Interface Sci., 547, 2019, 407-420. https://doi.org/10.1016/j.jcis.2019.03.098
19. M.L. Lindstrom , R. Gakhar , K. Raja , D. Chidambaram, Facile synthesis of an efficient Ni-Fe-Co based oxygen evolution reaction electrocatalyst, J. Electrochem. Soc., 167, 4, 2020, 046507-0465507. https://doi.org/10.1149/1945-7111/ab6b08
20. Y. Wang, B. Ma, Y. Chen, Iron phosphides supported on three-dimensional iron foam as an efficient electrocatalyst for water splitting reactions, J. Mater. Sci., 54, 2019, 14872–14883. https://doi.org/10.1007/s10853-019-03985-9
21. Y. Pang, W. Xu, Shengli Zhu, Zh. Cui, Y. Liang, Zh. Li, Sh. Wu, Ch. Chang, Sh. Luo, Self-supporting amorphous nanoporous NiFeCoP electrocatalyst for efficient overall water splitting, J. Mater. Sci. Technol., 82, 2021, 96-104. https://doi.org/10.1016/j.jmst.2020.11.020.
22. J. Li, W. Xu, D. Zhou, J. Luo, D. Zhang, P. Xu, L. Wei, D. Yuan, Synthesis of 3D flower-like cobalt nickel phosphate grown on Ni foam as an excellent electrocatalyst for the oxygen evolution reaction, J. Mater. Sci., 53, 2018, 2077–2086. https://doi.org/10.1007/s10853-017-1631-3
23. A.A. El-Moneim, N. Kumagai, K. Hashimoto, Mn-Mo-W oxide anodes for oxygen evolution in seawater electrolysis for hydrogen production, Mat. Transactions, 50, 8, 2009, 1969-1977. https://doi.org/10.2320/matertrans.M2009107
24. L. Wu , L. Yu , F. Zhang , D. Wang , D. Luo , S. Song , C. Yuan , A. Karim , S. Chen , Z. Ren, Facile synthesis of nanoparticle-stacked tungsten-doped nickel iron layered double hydroxide nanosheets for boosting oxygen evolution reaction, J. Mater. Chem., A 8, 2020, 8096-8103. https://doi.org/10.1039/D0TA00691B
25. R.M. Neethu, A.C. Hegde, Development of Ni-W alloy coatings and their electrocatalytic activity for water splitting reaction, Physica B: Condensed Matter., 597, 2020, 412359. https://doi.org/10.1016/j.physb.2020.412359
26. R. Rashkov, Synthesis and characterization of novel electrodeposited catalytic materials for hydrogen evolution reaction, Bul. Chem. Com., 40, 3, 2008, 211-218.
27. V.D. Bachvarov, M.H. Arnaudova, R.St. Rashkov,

A. Zielonka, Electrochemical deposition of alloys based on Ni-Fe-Co, containing W, P and their characterization for hydrogen evolution reaction, Bul. Chem. Com., 43, 1, 2011, 115-119.

28. G. Borisov, V. Bachvarov, H. Penchev, R. Rashkov, E. Slavcheva, Multi-metallic electrodeposited catalysts applicable for oxygen evolution reaction in AEM water electrolysis, Mat. Lett., 286, 2021, 129248. https://doi.org/10.1016/j.matlet.2020.-129248.
29. V. Bachvarov, E. Lefterova, R. Rashkov, Electrodeposited NiFeCo and NiFeCoP alloy cathodes for hydrogen evolution reaction in alkaline medium, Int. J. Hydrogen Energy, 41, 30, 2016, 12762-12771. https://doi.org/10.1016/j.ijhydene.2016.05.164
30. Q. Zhang, D. Yan, Z. Nie, X. Qiu, S. Wang, J. Yuan, D. Su, G. Wang, Z. Wu, Iron-doped NiCoP porous nanosheet arrays as a highly efficient electrocatalyst for oxygen evolution reaction, ACS Appl. Energy Mater., 1, 2, 2018, 571-579. https://doi.org/10.1021/acsaem.7b00143
31. A.I. Krasil'shchkov, Intermediate stages of anodic oxygen evolution, Zh. Fiz. Khim., 37, 1963, 531-537.
32. J.O'M. Bockris, Kinetics of activation controlled consecutive electrochemical reactions: Anodic evolution of oxygen, J. Chem. Phys., 24, 1956, 817-825. https://doi.org/10.1063/1.1742616
33. B.M. Jović, U.Č. Lačnjevac, V.D. Jović, Lj. Gajić-Krstajić, J. Kovač, D. Poleti, N.V. Krstajić, Ni-(Ebonex-supported Ir) composite coatings as electrocatalysts for alkaline water electrolysis. Part II: Oxygen evolution, Int. J. Hydrogen Energy, 41, 45, 2016, 20502-20514. https://doi.org/10.1016/j.ijhydene.2016.08.226
34. E. Guerrini, M. Piozzini, A. Castelli, A. Colombo, S. Trasatti, Effect of FeO_x on the electrocatalytic properties of $NiCo_2O_4$ for O_2 evolution from alkaline solutions, J. Solid State Electrochem., 12, 2008, 363–373. https://doi.org/10.1007/s10008-007-0406-1